References

1. K. H. No and C. D. Gutsche, *J. Org. Chem.*, **47**, 2708 (1982).
2. (a) V. Bohmer, F. Marschollek, and L. Zetta, *J. Org. Chem.*, **52**, 3200 (1987); (b) H. Goldman, W. Vogt, E. Paulus, and V. Bohmer, *J. Am. Chem. Soc.*, **110**, 6811 (1988).
3. J.-D. van Loon, A. Arduini, W. Verboom, R. Ungaro, G. J. van Hummel, S. Harkema, and D. N. Reinhoudt, *Tetrahedron Lett.*, **30**, 2681 (1989).
4. K. H. No and M. S. Hong, *Bull. Korean Chem. Soc.*, **11**, 58 (1990) and *J. Chem. Soc. Chem. Commun.*, 572 (1990).
5. C. D. Gutsche, B. Bhawan, J. A. Levine, K. H. No, and L. J. Bauer, *Tetrahedron*, **39**, 409 (1983).
6. C. D. Gutsche and J. A. Levine, *J. Am. Chem. Soc.*, **104**, 2652 (1982).
7. (a) K. H. No, Y. J. Noh, and Y. H. Kim, *Bull. Korean Chem. Soc.*, **7**, 442 (1986); (b) K. H. No and Y. H. Kim, *ibid*, **9**, 52 (1988).
8. G. A. Sheldrick, SHELXS-86 and SHELX-76, A Program for Crystal Structure Determination. Univ. of Cambridge, England (1986, 1976).
9. H. R. Hall and J. M. Stewart, XTAL version 2.2, Univ. of Western Australia and Univ. of Maryland (1987).
10. W. Saenger, Ch. Betzel, B. Hingerty, and G. M. Brown, *Nature*, **296**, 581 (1982).
11. G. D. Andreetti, R. Ungaro, and A. Pochini, *J. Chem. Soc. Chem. Commun.*, 1005 (1979).

The Effect of Minimum Energy Path Curvature on the Dynamic Threshold for Collision-induced Dissociation

Kihyung Song

Department of Chemistry, Korea National University of Education, Chungbuk 363-791.
Received May 28, 1991

In this paper, the question whether the curvature of the minimum energy path can affect the dynamic threshold was tested using the boundary trajectory method developed by Chesnavich and coworkers. For nonreactive system, the MO EXP model potential surface was used with modified equilibrium distance to control the curvature. The results showed that there is no relation between the curvature and the dynamic threshold. In order to study the reactive system, a generalization of the boundary trajectory method was achieved to apply on the nonsymmetric system. We have found no correspondence between the curvature and the dynamic threshold of the system. It was also shown that the fate of the trajectories strongly depends on the shape of potential surface around the turning points along the symmetric stretch line.

Introdution

A series of studies of collision-induced dissociation (CID) has shown that the dynamic threshold for atom-diatom collisions on nonreactive potential surfaces is much larger than the energetic threshold, *i.e.*, the dissociation energy, whereas, for collisions on reactive surfaces, the thresholds nearly coincide[1-4]. An example of the former type is $He+H_2$ collisions and the latter is illustrated by $H+H_2$ collisions.

Bergeron *et al.*[1] suggested that the larger dynamic threshold is typical of nonreactive systems, and is an artifact of collinear model calculations. However, it has been shown that three dimensional systems can also show this behavior[3]. Hence, this behavior appears to be independent of the dimensionality of the system.

Dove *et al.*[3] have argued that the shape of the potential surface is the primary factor governing the behavior of the CID threshold. They noted that when a contour map of the potential energy for an A+BC type reaction is plotted aganinst the A−B and B−C distance, the minimum energy path from the reactant channel tends to curve upward at small A−B distance (toward longer B−C distance) for reactions with an exchange channel (to AB+C), while it curves down (toward shorter B−C distance) for the reactions without an exchange channel. This elongating or shortening of the B−C distance could enhance or reduce, respectively, the dissociation into B+C particles.

In this study, the effect of the shape of the potential surface on the CID threshold for the reaction.

$$H+H_2 \rightarrow H+H+H \quad (1)$$

is tested using model potentials which show both upward and downward curvature for reactive and non-reactive systems. A classical trajectory method for collinear model was used for this study. The effect of incoming particle's mass is also investigated by changing its mass from 1 to 4. The CID boudary method[5-7] is used to determine the dissociative band in the reactant phase space.

In Section II, model potential surfaces used for reactive and nonreactive systems are shown. The method of calculation is explained in Section III, including a brief review of the CID boundary method. Results of this study are presented with discussions in Section IV. A conclusive summary is given in Section V.

Model Potential Surfaces

Table 1. Parameters for Nonreactive Potential (in atomic units)

C	1.5	α	1.2376
D	0.12012	$R_{2_0}^0$	1.402
λ	0.37142		

Table 2. Parameters for Reactive Potential (in atomic units)

D	0.12012	s	0.1	($\beta=0$)
R_0^0	1.402		0.2	($\beta=-1$)
α	1.2376		0.066	($\beta=1$)

In order to study the relationship between the dynamic threshold and the curvature of the minimum energy path on the potential energy surface, it is necessary to construct model potentials for which the curvature can be controlled easily. Both systems with and without an exchange reaction channel are considered.

There are many potential surfaces used for the reaction (1)[8], including the Porter-Karplus No. 2 (PK2H3) surface[9], which has been used widely for trajectory studies of this system[5-8]. However, due to the complexity of this surface, it is hard to control the shape of the surface with simple parametric equations. Also, it is useful if we have a similar functional form for both reactive and nonreactive systems. We chose a model potential, used by Bergeron *et al.*[1], consisting of a Morse diatomic interacting with an incoming atom through an exponentially repulsive potential (MO EXP model) for the nonreactive system, and a London-Eyring-Polanyi-Sato (LEPS) potential[10,11] for the reactive system. Both use the Morse potential, which can be easily modified to produce the changes in curvature.

Nonreactive System. For nonreactive systems, the MO EXP model potential surface used by Bergeron *et al.*[1] is used. This potential energy is the sum of two parts :

$$V(R_1, R_2)=V_1+V_2 \tag{2}$$

where V_1 is an exponentially repulsive potential,

$$V_1=C\exp(-\lambda^{-1}R_1), \tag{3a}$$

and V_2 is a Morse potential,

$$V_2=D\{\exp[-\alpha(R_2-R_2^0)]-1\}^2-D \tag{3b}$$

Here R_1 and R_2 represent the A−B and B−C distances, respectively. In order to produce the necessary positive and negative curvature on the minimum energy path, R_2^0 is set to be a function of R_1 :

$$R_2^0(R_1)=R_{2_0}^0[1+\beta\exp(-R_1)] \tag{4}$$

The same values for parameters, C, D, λ, α, and $R_{2_0}^0$ are used as in ref. 7, and are given in Table 1. The coefficient β controls the direction of curvature. Positive curvature can be obtained by a positive β, and negative β gives a negative curvature. The unmodified surface can be obtained by setting $\beta=0$.

Figure 1 shows contour plots on the mass-weighted skewed coordinate, (x, y) plane of the potential surface with β equal to 0, −1, and 1. The definitions of (x, y) coordinates are given in ref. 5 and other texts on scattering theories.

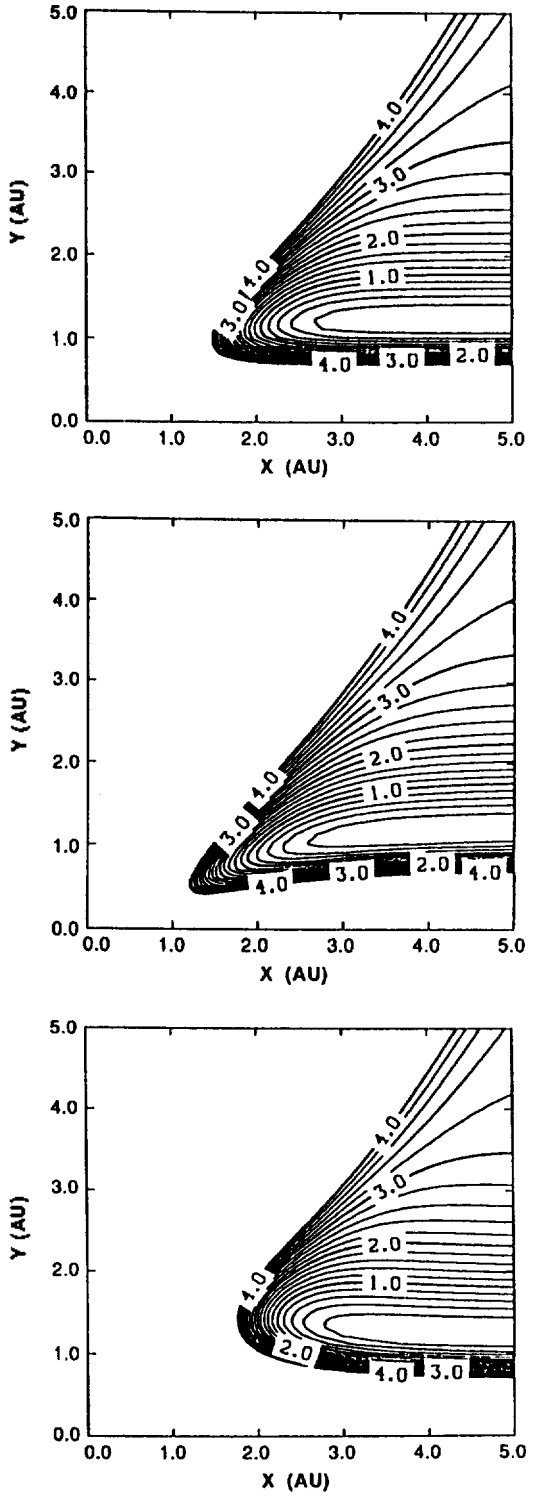

Figure 1. Contour plot for the potential energy surface used for nonreactive system in the (x, y) coordinate system. In this and all contour plots in this paper, energies are in units of eV. (a) No modification ($\beta=0$). (b) Negative curvature ($\beta=-1$). (c) Positive curvature ($\beta=+1$).

The minimum energy path of the unmodified surface (Figure 1a) shows slightly downward curvature. This curvature is enhanced by a negative β value (Figure 1b). Figure 1c shows the curvature shifting upward with $\beta=1$. The simple para-

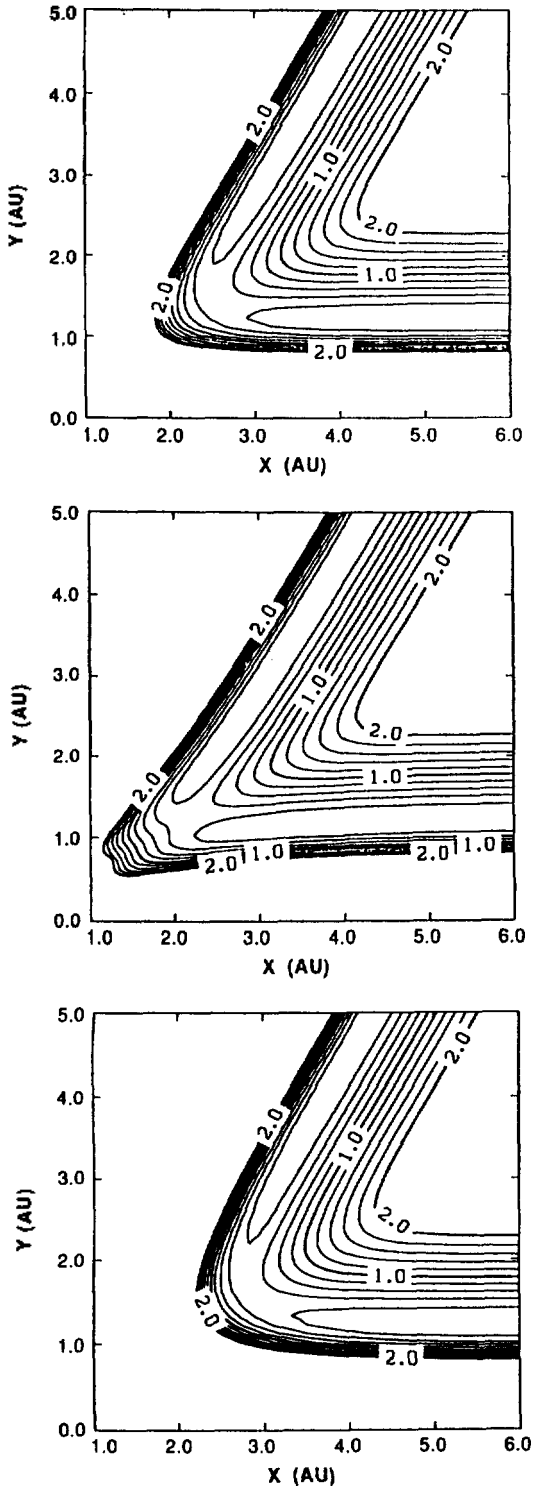

Figure 2. Contour plot for the potential energy surface used for the reactive system in the (x, y) coordinate system. (a) No modification ($\beta=0$). (b) Negative curvature ($\beta=-1$). (c) Positive curvature ($\beta=+1$).

meterization of the equilibrium distance using Eq. (4) can give both negative and positive curvatures on the minimum energy path curve.

Reactive System. A LEPS potential[10,11] is used for the reactions with an exchange channel. Inorder to control the curvature, the equilibrium distances in the expressions for both Morse and "anti-Morse" potentials are changed as a function of the other distances, using the same functional form as Eq. (4). Due to the symmetry of the $H+H_2$ system, the same constant β is used for both R_1 and R_2. Also, the same parameters D, α, R_0^0, and s are used for the potentials of all three pairs, and are given in Table 2. Note that, in order to keep the barrier heght, $E_0=0.31$ eV (value for $\beta=0$ case), for all three values of β, the value of the Sato parameter s is changed accordingly. These parameters are also given in Table 2.

The contour plots of the potential energy surfaces in the (x, y) coordinate system are given in Figure 2, with $\beta=0, -1$, and 1. Figure 2a is an unmodified LEPS surface. This shows slightly upward curvature, starting at $x\approx 3.0$ a.u., on the minimum energy path curve. As shown in Figure 2b, the surface with $\beta=-1$ gives negative curvature until $x\approx 2.2$ a.u. A positive β value (Figure 2c) gives earlier turning of the minimum energy path curve, starting at $x\approx 4$ a.u., toward higher values of y. Hence the same modification of the equilibrium distance using Eq. (4) can produce negative and positive curvature for both reactive and nonreactive potential surfaces.

Method of Calculation

In this study, the CID boundary method[5-8] is used to determine the dissociative band in the reactant channel as a function of the total energy. Detailed discussions on this method appear elsewhere[5,6]. Hence, only a brief description for this method is given in Section 1. This method has been applied only to reactions with a symmetric reactive system[5,8]. How to apply this method to various types of reactions, *i.e.*, nonreactive (Section 2) and reactive (Section 3) systems is discussed. In Section 3, it is shown that the CID boundary method can also be applied to nonsymmetric systems using some simple strategies.

Method of Boundary Trajectories. In the atom-diatom reaction, at time $t\rightarrow\infty$, the product atom and diatom are well separated. Hence, the system's Hamiltonian can be separated into H_d, the Hamiltonian of the product diatom, and H_t, the Hamiltonian for free translational motion of the atom-diatom pair. The product diatom can be divided into two categories : the dissociative trajectories which have $H_d>D$, the dissociation energy, and the nondissociative bound trajectories, which have $H_d<D$. These two sets of trajectories are divided by the trajectories with $H_d=D$. If the trajectories are run backwards from the final states with the boundary condition $H_d=D$ and $t\approx\infty$, the conditions in the reactant states, $t=0$, will give the boundaries of the dissociative bands. If the trajectories are initiated from the product, channel the boundary is between the reactive and the dissociative bands. Otherwise, if the trajectories start from the reactant channel, they form the nonreactive-dissociative boundaries. Note that, these trajectories are run backwards in time.

In the mass-weighted skewed coordinate system,* the Hamiltonian can be written as

$$H=\frac{p_x^2+p_y^2}{2\mu}+V(x, y), \tag{5}$$

where V is the potential energy and $\mu=m_A(m_B+m_C)/M$ is the reduced mass of the system, and M is the total mass, $m_A+m_B+m_C$. Note that, Eq. (5) is the equation of motion for a single particle with mass μ moving in the (x, y) plane. The diatomic energy, H_d, at a given x and y, is defined by

$$H_d=\frac{p_r^2}{2\mu}+V(x, y) \tag{6}$$

Eq. (5) is integrated to get the trajectories. With H_d set equal to D, the trajectories are initiated from the surface with large enough x ($x=20$ a.u. is chosen) and initial p_r as determined by Eq. (6). The initial value of p_{x_i} is calculated by the total Hamiltonian, Eq. (5). The sign of p_{x_i} is set to be negative so that the trajectories move inward. Both positive and negative values of p_{x_i} are used, but it was found that no value of $p_{x_i}>0$ leads to the bound states at final points. When the trajectories are collected in the reactant region, the transformation from (y, p_y) to the action-angle pair (n, θ) is done by the expressions in ref. 5.

Nonreactive System. For a system with no exchange channel, there are two possible outcomes: A+BC→A+BC or A+B+C. Since there is no 'product' channel for this type of system, one surface at large x (say, $x=20$ a.u.) can serve as both the initiation and collection surface for initial and final conditions of the trajectories. For this surface, a line is drawn at $x=20$ a.u. in Figure 2. The values for the initial y coordinates are then chosen on this line between the two solutions of $V(20, y)=D$. A collection of final conditions is made for the trajectories passing this line again with diatomic energies less than the dissociation threshold.

Reactive System

Symmetric System. In the case of a symmetric system, such as $H+H_2$, the possible reaction channels are

$$H+H_2\rightarrow\begin{cases}H+H_2 & \text{(Nonreactive)}\\ H_2+H & \text{(Reactive)}\\ H+H+H & \text{(Dissociative)}\end{cases} \tag{7}$$

Note that the reactive and nonreactive channels are identical. Also, the reactant and product channels can be divided by the symmetric stretch line. Hence, the trajectory point in the product channel, *i.e.*, above the symmetric stretch line in the x-y plane, is identical to the trajectory point in the reactant channel, when they are symmetric to each other with respect to the symmetric stretch line. The reactant channel is taken to be the channel for which motion along x as $x\rightarrow\infty$ corresponds to relative translational motion of the atom-diatom pair, and motion along y corresponds to vibration of the diatom.

The transformation between the reactant and product channel coordinates can be done using the following transformation matrix $\underline{\boldsymbol{P}}$:

$$\underline{\boldsymbol{P}}=\begin{pmatrix}\cos\beta & \sin\beta\\ \sin\beta & -\cos\beta\end{pmatrix} \tag{8}$$

where the skew angle β is defined in ref. 5. Note that the matrix $\underline{\boldsymbol{P}}$ is independent of the angle of the symmetric stretch line.

The integration of trajectories is done until they either recross the $x=20$ a.u. surface or cross the equivalent surface in the product channel. The nonreactive-dissociative (ND) boundaries are obtained from the trajectories that recross the initial surface in the reactant channel simply by changing the sign of p_y at the point at which they cross. The reactive-dissociative (RD) boundaries are obtained from the trajectories that crossed the product channel surface by taking the point at which they crossed and reflecting it through the symmetric stretch line to obtain the equivalent point on the reactant channel surface, and then changing the sign of the resulting value of p_y. Only the bound trajectories with diatomic energy less than the dissociation energy are collected for the boundaries.

Nonsymmetric System. When the mass of the incoming particle is changed from 1 to 4, the reaction (1) becomes nonsymmetric, in which the reactant and product channels are no longer equivalent. In this case, the trajectories should be initiated from the appropriate channel: *i.e.*, from the reactant channel for ND boundaries, and from the product channel for RD boundaries. This is because the main idea of the boundary trajectory method is to run the trajectories from the final channel to the initial channel. Hence it is necessary to run the trajectories from the true final channels.

In general, the symmetric stretch line, defined in the symmetric case, no longer has a physical significance in the nonsymmetric case. However, it is necessary to determine a line which separates the reactant and product channel. This can be done by determining the maximum point on the potential surface at constant x, for x values up to a maximum, say, $x=20$ a.u. In this study, however, only the mass of the incoming particle is changed from 1 to 4, and the potential surface is not changed, the same symmetric stretch line (with a different slope on the x-y surface) can be used.

The initial points for the ND boundary trajectories can be obtained by the same method as for the symmetric system since the trajectories are initiated from the surface in the reactant channel. The collection of the ND boundaries, however, should be made from the trajectories coming out to the reactant channel surface. The trajectories which come out to the product channel are ignored, unless both forward and reverse reactions are studied simultaneously.

For the RD boundaries, an initial x value is determined by transforming the point $(20, y_s)$,where y_s is the maximum point of the potential energy at $x=20$ a.u., to the reactant channel, using Eq. (8). The value of x_i is then set equal to the transformed x coordinate of the point $(20, y_s)$. The values of y_i are chosen as usual. Then the point (x_i, y_i) is tranformed back to the product channel point (x_p, y_p). The value of p_{y_i} is calculated using the potential energy, $V(x_p, y_p)$, instead of $V(20, y_i)$. Now, p_{x_i} is calculated from the total energy. The momentum pair (p_{x_i}, p_{y_i}) is then transformed to the product channel momenta (p_{x_p}, p_{y_p}). The trajectories are run from the phase space point $(x_p, y_p, p_{x_p}, p_{y_p})$. Note that, for symmetric systems, these transformations do not affect the trajectory due to the symmetry. The RD boundary points are collects from the trajectories coming out to the reactant channel. Again, the trajectories coming out to the product channel are discarded.

Results and Discussion

In this study, trajectories are run with fixed total energy,

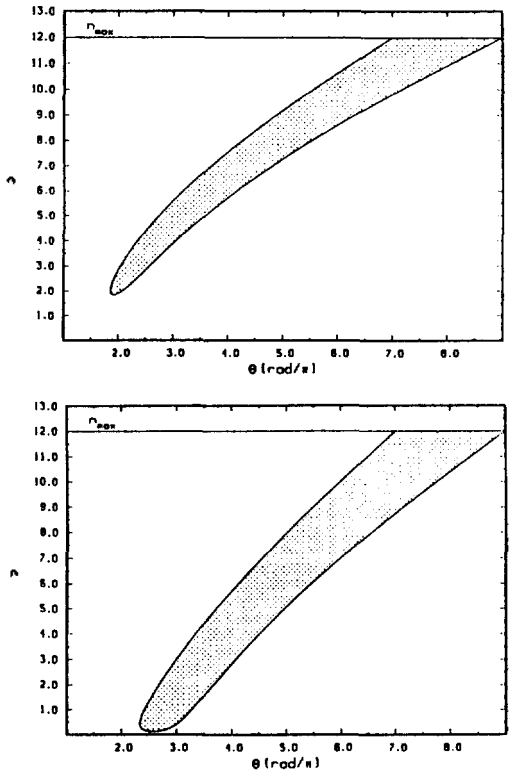

Figure 3. The action-angle plot of the dissociation band for the $H+H_2$ nonreactive system with no modification ($\beta=0$). (a) $E=$ 2.18 eV above threshold. The shaded area is the dissociative band and the unshaeded area is the nondissociative condition. (b) $E=4.90$ eV above threshold.

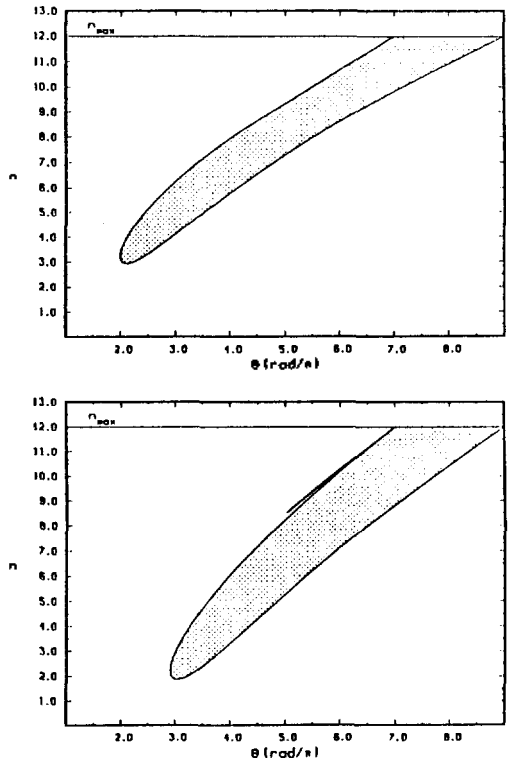

Figure 4. The action-angle plot of the dissociation band for the $H+H_2$ nonreactive system with negative curvature ($\beta=-1$). (a) $E=2.18$ eV above threshold. (b) $E=4.90$ eV above threshold.

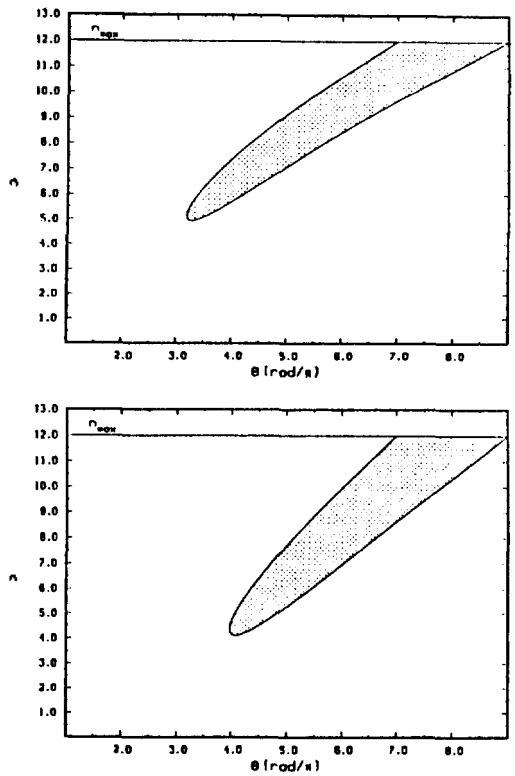

Figure 5. The action-angle plot of the dissociation band for the $H+H_2$ nonreactive system with positive curvature ($\beta=+1$). (a) $E=2.18$ eV above threshold. (b) $E=4.90$ eV above threshold.

Most trajectory studies are done with fixed relateve translational and vibrational energies[1-4]. However, the result of this study can be used to obtain the results with fixed translational and vibrational enegy. For example, the example, the dissociation probabilities as a function of translational and vibrational energies can be obtained from the action-angle plot of a dissociative band as follows. First, the dissociation probability at a certain vibrational state n and total energy E can be calculated from the horizontal width of the dissociative band at action equal to $n+1/2$, divided by the length of 2π on the angle axis. The translational energy can be obtained from the fact that, for collinear systems, the total energy is the sum of diatomic vibrational and relative translational energies.

Using the CID boundary method, the dynamic threshold for the reactant vibratioanl state n can be obtained by detemining the total energy, below which the dissociative band does not reach the specific action, $n+1/2$, and above which the band reaches lower action than $n+1/2$. In this study, the dissociative bands were obtained at a fixed energy for all three curvatures. The lowest action of the dissociative band for each curvature is compared. If, for example, the lowest action for negative curvature is higher than that of positive curvature, it can be concluded that the positive curvature enhances the dissociation process, as stated in ref. 3. Calculations were performed for both nonreactive and reactive potential surfaces with masses of 1-1-1 and 4-1-1.

Nonreactive System. In Figures 3-5, the calculated dissociation bands for energies equal to 2.18 eV (a) and 4.90 eV (b) above threshold are shown for the potential surface

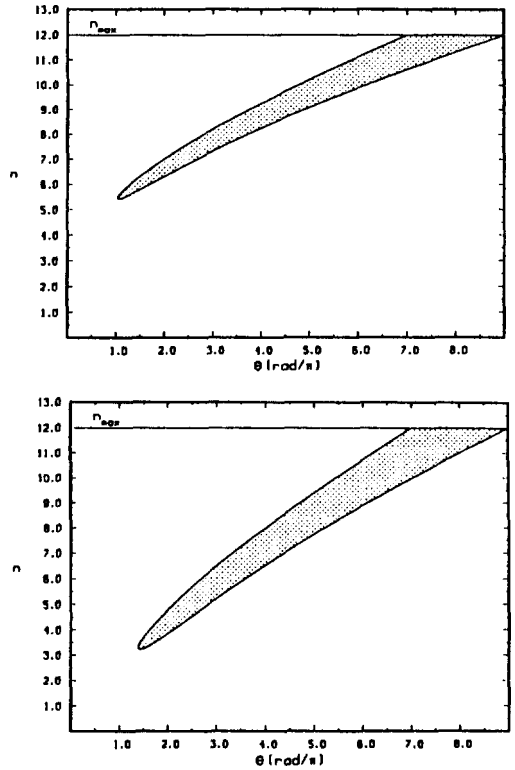

Figure 6. The action-angle plot of the dissociation band for the $H+H_2$ nonreactive system with no modification ($\beta=0$) for 4-1-1 masses. (a) $E=2.18$ eV above threshold. (b) $E=4.90$ eV above threshold.

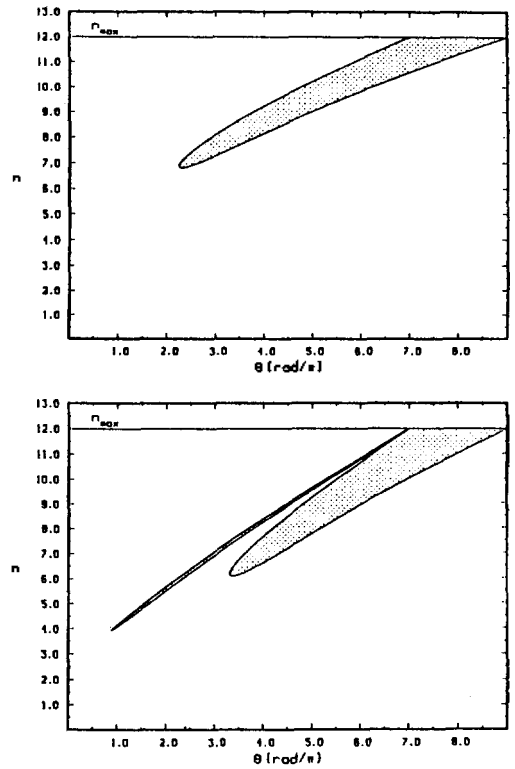

Figure 7. The action-angle plot of the dissociation band for the $H+H_2$ nonreactive system with negative curvature ($\beta=-1$) for 4-1-1 masses. (a) $E=2.18$ eV above threshold. (b) $E=4.90$ eV above threshold.

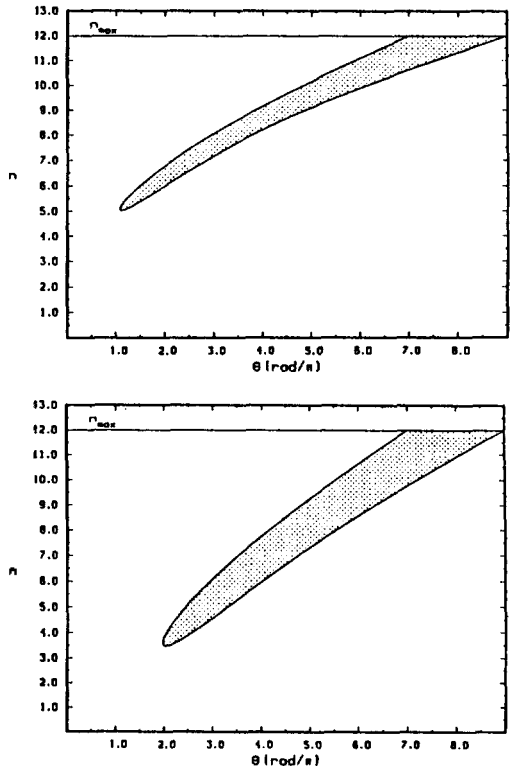

Figure 8. The action-angle plot of the dissociation band for the $H+H_2$ nonreactive system with positive curvature ($\beta=+1$) for 4-1-1 masses. (a) $E=2.18$ eV above threshold. (b) $E=4.90$ eV above threshold.

with no modification (Figure 3), negative (Figure 4), and positive (Figure 5) curvatures. These energies are equal to $\hbar\omega$ and $15\hbar\omega(1\hbar\omega=0.54486$ eV), respectively, in the unit used in ref. 1. For every curvature, the higher energy can produce dissociation at a lower vibrational state. Note that, for both energies, the dissociation bands with no modification (Figure 3) extend to the lowest value of n. Also, the bands with negative curvature (Figure 4) reach lower n value than those with positive curvature (Figure 5). This means that the negative curvature produces lower dynamic threshold than the positive curvature. Since, at $E=2.18$ eV above dissociation threshold, none of the dissociation bands reaches the $n=1/2$ state, (See Figures 3a, 4a, and 5a) the dynamic threshold for all three curvatures is much higher than the energetic threshold.

Comparison of our results to the classical dissociation probability given in Figure 1a of ref. 1, was also made. The dissociation probability, for example, of the $v=3$ state at $E_{tot}=10\hbar\omega$ ($=2.18$ eV above threshold) was obtained from the band width at $n=3+1/2$ divided by the length of 2π in Figure 3a. Probabilities obtained from both Figures. 3a and 3b gave excellent agreement.

In order to investigate the effect of the mass of an incoming particle, calculations were also carried out with masses of 4-1-1 using the same potential surface. The results are shown in Figs. 6-8, with the same total energies and curvatures. In this case, the curvature which produces dissociation with the lowest action is different for each energy. At $E=$ 2.18 eV above threshold, the surface with positive curvature

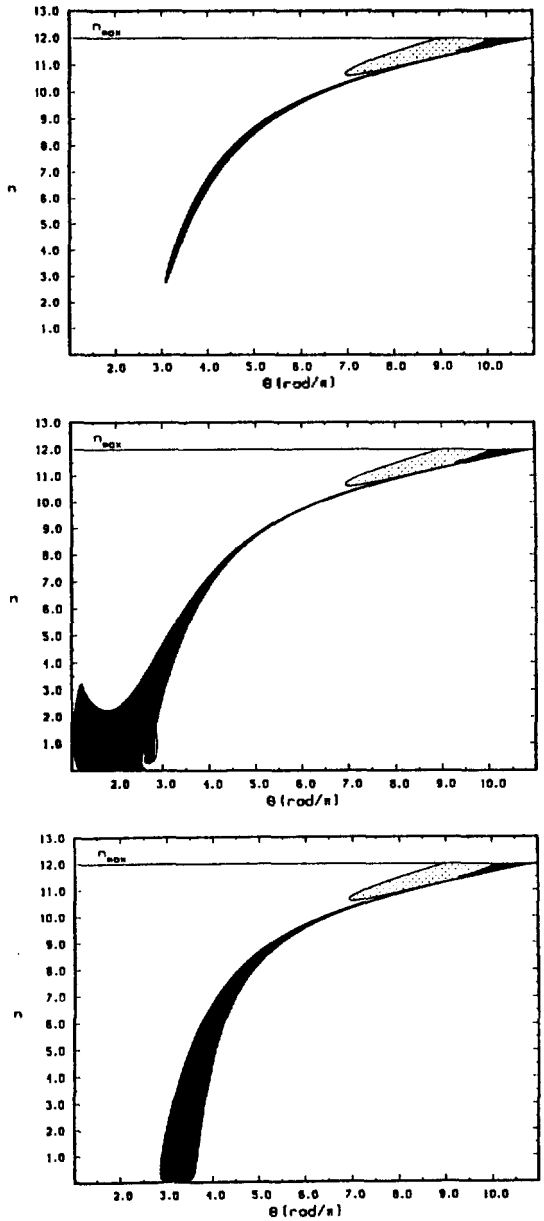

Figure 9. The action-angle plot of the reactive (black), dissociative (dotted), and nonreactive (white) bands for the $H+H_2$ with reactive LEPS potential. The total energy of the system is set equal to 0.1 eV above threshold. (a) No modification. The black area is the reactive band, the dotted area is the dissociative band, and the unshaded area is the nonreactive band. (b) Nigative curvature. (c) Positive curvature.

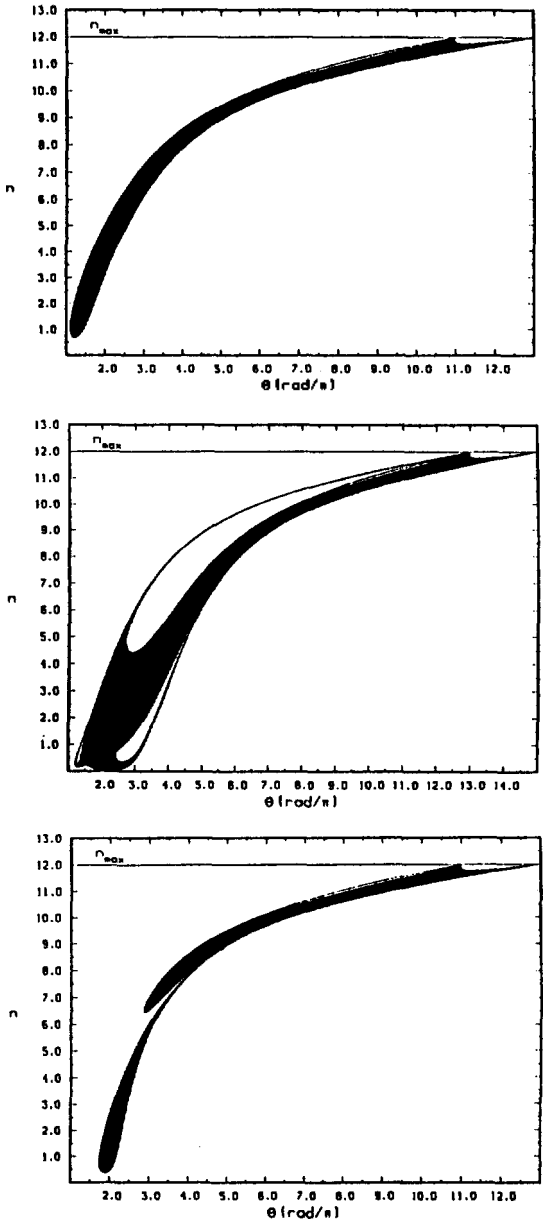

Figure 10. The action-angle plot of the reactive (black), dissociative (dotted), and nonreactive (white) bands for $H+H_2$ with reactive LEPS potential for 4-1-1 masses. The total energy of system is set equal to 0.1 eV above threshold. (a) No modification. (b) Negative curvature. (c) Positive curvature.

(Figure 8a) yields dissociation at a little lower action than with no modification (Figure 6a), while at $E=4.90$ eV, the surface with no modification (Figure 6b) gives the lowest action. At both energies, the positive curvature (Figure 8) produced dissociation at lower action than the negative curvature (Figure 7). Changing the mass of the incoming atom from 1 to 4 gives different behavior about the change of the dynamic threshold with different curvature. This mass of the incoming particle also shows the dynamic threshold is much higher than the energies threshold, for all curvatures.

One interesting feature is that, negative curvature gives two dissociation bands at $E=4.90$ eV, for both the 1-1-1 (Figure 4b) and 4-1-1 (Figure 7b) masses. The narrow band of the 1-1-1 masses is much smaller than that of the 4-1-1 masses. As shown in Figure 7b, the narrow band extends to much lower action than the wide band. We are not sure what causes this pattern. Since, in this study, our main purpose is to determine the dynamic threshold, we made no further investigation on this two-band structure.

Reactive System. A reactive potential surface was modeled using the LEPS potential[8,10,11]. Parameters were kept equal to those of the nonreactive system as much as possible, including the method of changing the curvature. The total

energy of the system was set equal to 0.1 eV above threshold. The results for the 1-1-1 system are shown in Figure 9. The shape of Figure 9a looks very similar to the results of the $H+H_2$ system using the PK2H3 potential surface[9], in ref. 6. This is due to the fact that the shape of the unmodified LEPS surface is similar to the PK2H3 surface.

In Figure 9, the reactive bands (black area) are surrounded by a dissociative band, which is not visible for the low-action band[5-7]. The lowest action of the dissociative band with the unmodified LEPS surface is ≈ 2.5 as shown in Figure 9a. Both negative (Figure 9b) and positive (Figure 9c) curvature intensified the low action region, and lowered the lowest action down to almost 0. This means that, the dynamic threshold for the unmodified surface is higher than 0.1 eV above energetic threshold and that for both negative and positive curvatures it is lower than 0.1 eV above the energetic threshold.

The surface with negative curvature produced a very complex band structure, as shown in Figure 9b. This is due to the irregular shape of the surface around the turning point, *i.e.*, the point where the trajectory bounces from the potential energy surface, along the symmetric stretch line of the potential surface, shown in the lower left hand corners of Figure 2b. In the unmodified surface (Figure 2a), the shape of contour lines around this area have simple curvature. Figure 2b shows a 'hump' around that point. As stated in ref. 6, the trajectories which follow the symmetric stretch line near the turning point are extremely sensitive to the initial condition. Hence, the complexity of the plot for the negative curvature is due to the irregularity around the turning point on the symmetric stretch line of the potential surface.

The results for the same potential surfaces with 4-1-1 masses are plotted in Figure 10. The shape of the bands are very different from that of the system with 1-1-1 masses. Note that the only difference between the two systems is the mass of the incoming atom. Other parameters are kept equal, including the total energy. For the systems with no modification, the main difference between the systems with the 1-1-1 and 4-1-1 masses is that the narrow low action band in the 1-1-1 system gets bigger in the 4-1-1 system to surround the dissociation band in the high action region. This appears for all curvatures. As in the 1-1-1 system, the bands for both positive and negative curvatures reach down to lower action than those with no modification. Again, the band structure of the negative curvature is very complex due to the irregular shape of the model potential. Since the dissociative bond goes down to $n \approx 0.5$, the ground state for the unmodified surface (Figure 10a), and lower than 0.5 for both negative (Figure 10b) and positive (Figure 10c) curvatures, the dynamic threshold for these systems is close to $D+0.1$ eV. In the mass effect study of quantum mechanical CID by Kaye and Kuppermann[12], they also stated that the dynamic threshold is close to the energetic threshold, for all the mass combinations studies.

Conclusions

Dove *et al.*[3] speculated that the negative curvature of the minimum energy path reduces the diatomic distance as the incoming atom approaches, while the positive curvature makes it increase. The increase of diatomic distance could enhance the dissociation process and the compression could make dissociation difficult. However, this study reveals almost no correlation between the curvature of the minimum energy path and the dynamic threshold. In agreement with other results[1-4], the above results also show that the dynamic threshold of a nonreactive system is much higher than that of a reactive system. From the results of this study, it is concluded that the curvature of the minimum energy path is not the major reason why the dynamic threshold is much higher than the energetic one for the nonreactive systems.

Instead of the diatomic interacion[3], it would be appropriate to focus on the interaction between the diatom and the incoming atom. If there is an exchange channel, the force between the incoming atom and one atom of the diatom is attractive. Hence it would withdraw the atom from the diatom. This could boost both the dissociation and reaction processes. In the case of a nonreactive system, the interaction is repulsive. This could cause the diatom to retract and hence makes dissociation difficult. Therefore, we suggest that the main cause of the difference of dynamic threshold between reactive and nonreactive systems is not the curvature of the minimum energy path on the potential surface, but the presence of the exchange channel.

References

1. G. Bergeron, P. C. Hiberty, and C. Leforestier, *Chem. Phys.*, **93**, 253 (1985).
2. C. Leforestier, *Chem. Phys. Lett.*, **125**, 373 (1986).
3. J. E. Dove, M. E. Mandy, N. Sathyamurthy, and T. Joseph, *Chem. Phys. Lett.*, **127**, 1 (1986).
4. N. C. Blais and D. G. Truhlar, in *Potential Energy Surfaces and Dynamics Calculations*, edited by D. G. Truhlar (Plenum, New York, 1981), p. 431
5. M. E. Grice, Ph. D. Dissertation, Texas Tech University, 1987.
6. B. K. Andrews and W. J. Chesnavich, *Chem. Phys. Lett.*, **104**, 24 (1984).
7. M. E. Grice, B. K. Andrews, and W. J. Chesnavich, *J. Chem. Phys.*, **87**, 959 (1987).
8. A. D. Jorgensen, E. A. Hillenbrand, and E. A. Gislason, in *Potential Energy Surfaces and Dynamics Calculations*, edited by D. G. Truhlar (Plenum, New York, 1981), p. 421.
9. R. N. Porter and M. Karplus, *J. Chem. Phys.*, **40**, 1105 (1964).
10. S. Sato, *J. Chem. Phys.*, **23**, 592 (1955).
11. P. J. Kuntz, in *Dynamics of Molecular Collisions, Part B*, edited by W. H. Miller (Plenum Press, New York, 1976), p. 53.
12. J. A. Kaye and A. Kuppermann, *Chem. Phys.*, **125**, 279 (1988).